EFFECT OF ADDITIVES ON THE Al DIFFUSION BEHAVIOR IN UMo BASED FUELS

Jorge E. Garcés
Centro Atómico Bariloche, CNEA, 8400 Bariloche, Argentina

Guillermo Bozzolo
Ohio Aerospace Institute, 22800 Cedar Point Rd., Cleveland, OH 44142, USA

Gerard Hofman and Jeffrey Rest
Argonne National Laboratory, 9700 S. Cass Ave., Argonne, IL 60439, USA

ABSTRACT

In this work we apply an atomistic modeling tool for dealing with interfacial phenomena and the effects of selected additives in the behavior of the Al/UMo interface. The basic features characterizing the real system are identified in this modeling effort such as: the increased Al and U interdiffusion with temperature, the Al stopping power of increasing Mo concentration, and the formation of interfacial compounds. Moreover, significant results were also obtained in the case of Si additions to Al, once again reproducing the main features observed experimentally: the trend indicating formation of interfacial compounds, much reduced diffusion of Al into UMo due to the high Si concentration, Si depletion in the Al matrix, and an unexpected interaction between Mo and Si which avoid the Si diffusion to deeper layers in the UMo solid solution thus improving the stopping power for Al diffusion. The effects of other additives, such as Ge, are also discussed in the present work.

1. Introduction

Research and development programs based on the synergy between theory, modeling, and experiment, are growing both in number and strength. Their growth, however, relies heavily on a number of factors which favor certain fields of research more than others, as the theoretical complexities, the availability of computational modeling tools, and the ease to acquire experimental evidence rarely converge to provide a uniform platform for any given program, thus limiting the added value that arises from an optimum balance between them. One area of relevance where this is apparent is in the development of nuclear fuels for research and test reactors that meet current needs and concerns at a global scale.

The development of high density U-alloys with an increased concentration of U is one of the key ingredients for high neutron flux research reactors with low enriched uranium (LEU, ^{235}U < 20 at%) fuel. Of particular interest is the UMo solid solution in the γ-phase dispersed in an Al matrix or in a monolithic form, which generated high expectation due to its acceptable irradiation behavior, low to moderate fuel/matrix interaction, and stable fission gas bubble growth for moderate neutron fluxes. However, unexpected failures like pillowing and large porosities in high neutron fluxes irradiation experiments have been reported, probably due to the formation of ternary compounds and large porosity located at the interface between the interaction product and the Al matrix under high power operating conditions [1-3].

Several basic issues must be addressed in order to have a better understanding of the causes of the failures and the fundamental behavior of the different fuels as, for example, the processes involved in the interaction between the aluminum matrix and the UMo solid solution, or the interdiffusion or interfacial reaction with the Al matrix or cladding. Other basic questions relate

to the role of new additives in the stability of the bcc phase, as well as their influence on the thermal compatibility with the Al matrix and on potential porosity formation.

The complexities associated to each one of these questions require a considerable improvement to the traditional method for developing or improving specific alloys mostly based on extensive experimental trial and error work, which is both expensive and time-consuming. Recently, however, the increasing role of atomistic computational modeling in the development of structural materials has shown promise as a valuable tool to aid the experimental work. If theoretical modeling could also be included in the development of nuclear fuels, then the experimental process could be better directed and experiments could be reduced to specific ones correlated in number and nature to the guidance provided by the theoretical predictions.

While the virtual design of new materials through complex computer simulations is yet a goal to be achieved, its success will depend on the availability of a unified approach that provides the same level of simplicity and accuracy for any possible application. Although first-principles (FP) approaches provide the most accurate framework for such studies, the complexity of the tasks involving actinides and their substantial computational requirements impose limitations that still prevent these approaches from becoming economical predictive tools. In fact, the theoretical description of actinide metals and their alloys poses a severe challenge to modern electronic structure theory and has eluded accurate treatment by semiempirical or quantum approximate methods (qam). The purpose of qam is to provide an efficient and accurate way to compute the energy of arbitrary atomic systems in terms of their geometrical configuration in an economical computational way. Almost independently of their foundation and formulation, these methods rely on simplifications which, as a result, inevitably require the introduction of parameters that in some cases limit their use due to nontransferability problems that exist in their formulation.

A recently developed qam is the Bozzolo-Ferrante- Smith (BFS) method for alloys [4], which fulfills several requirements for applicability in terms of simplicity, accuracy, and range of application, as it has no limitations in its formulation on the number and type of elements present in a given alloy. Moreover, it has shown promise in describing diverse problems, particularly in the area of surface alloys [4] and high-temperature intermetallics [5-7]. The purpose of this work is then to apply the BFS method for describing the basic features observed in nuclear fuels that are currently under development with the aim to understand the basic behavior of each one of their components. A brief description of BFS method is presented in section 2 while section 3 shows the modeling results, obtained through Monte Carlo (MC) simulations, on the role of additives such as Si and Ge in the interface Al-U and Al-UMo systems. Conclusions are presented in Section 4.

2. The BFS method for alloys

The BFS method replaces the exact process of alloy formation with two virtual processes where the end result is, or is expected to be, a good description of the result of the real process. Thus, it is expected that BFS reproduces the essential features of the equation of state of the solid at zero temperature and, in particular, around equilibrium providing structural information that is ultimately, contained in the binding energy curve describing the solid under study. Basically, the BFS method provides a simple algorithm for the calculation of the energy of formation ΔH of an arbitrary alloy (the difference between the energy of the alloy and that of its individual constituents), written as the superposition of elemental contributions, ε_i, of all the atoms in the

alloy, where ε_i denotes the difference in energy between a given atom in the equilibrium alloy and in an equilibrium single crystal of species i, $\Delta H = \sum_i \varepsilon_i$.

In principle, the calculation of ΔH would simply imply computing the energy of each atom in its equilibrium pure crystal and the total energy in the alloy. In BFS, a two-step approach is introduced for the calculation of ε_i in order to identify contributions to the energy due to structural and compositional effects computed as isolated effects. Therefore, ε_i is broken up in separate contributions, each one related with a corresponding equivalent crystal (EQ): 1) a strain energy (ε^S) that accounts for the change in energy due *only* to the change in geometrical environment of the crystal lattice, ignoring the additional degree of freedom introduced by the varying atomic species in the alloy, 2) a chemical energy (ε^C), and 3) a chemical reference energy (ε^{Co}), where these last two terms take into account the real chemical enviroment in the alloy and decoupling between structural and chemical effects, respectively. It is precisely in the BFS chemical energy where the set of parameters describing the pure element are perturbed in order to account for the distortion introduced by the nearby presence of a different element or defect. While there is a certain level of arbitrariness in how this separation is implemented, it is only meaningful when a good representation of the initial and final states of the actual process is obtained by properly linking all contributions. This is achieved by recoupling the strain, chemical and chemical reference contributions by means of a coupling function, g_i, properly defined to provide the correct asymptotic behavior of the chemical energy contribution. Summarizing, the contribution to the energy of formation of atom i is then $\varepsilon_i = \varepsilon_i^S + g_i\left(\varepsilon_i^C - \varepsilon_i^{C_0}\right)$.

It can be shown that BFS predictions that result from this scheme are *identical* to FP calculations at or near equilibrium of the system under study, as shown in Fig. 1 for UMo B2 and the Ni_2AlTi Heusler alloy [8].

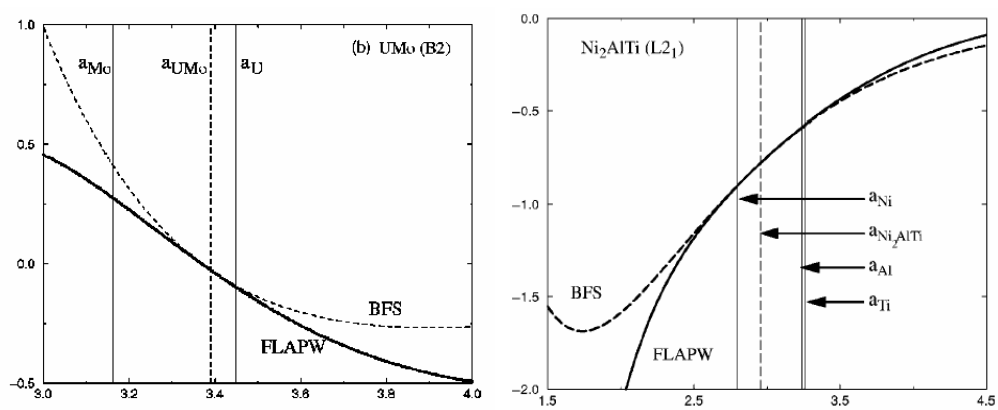

Figure 1. Comparison of the FLAPW results (solid curves) and BFS predictions (dashed curves) for the difference between the total energy and strain energy (in eV/atom) as a function of lattice parameter (in angstroms) for UMo *B*2 and Ni_2AlTi $L2_1$ structures. The vertical lines denote the equilibrium lattice parameters of the individual elements (in the symmetry of the alloy, dashed line) and the lattice parameter of each ordered structure (solid lines), as predicted by first-principles methods.

From a computational standpoint, the usefulness of the method relies on the simplicity of the calculations needed for the determination of the three EQ associated with each atom i. The procedure involves the solution of a simple transcendental equation for the determination of the equilibrium Wigner-Seitz radius (r_{WSE}) of each EQ. The BFS strain energy contribution, ε^S, is obtained by solving the Equivalent Crystal Theory [9] (ECT) perturbation equation

$$NR_1^p e^{-\alpha R_1} + MR_2^p e^{-(\alpha+1/\lambda)} = \sum_k r_k^p e^{-(\alpha+S(r_k))r_{kj}} \quad (1)$$

while the BFS chemical energy is obtained by a similar procedure by solving the equation

$$NR_1^{p_i} e^{-\alpha_i R_1} + MR_2^{p_A} e^{-(\alpha_i+1/\lambda_i)} = \sum_k r_1^{p_i} e^{-(\alpha_i+\Delta_{ki})r_1} + \sum_k r_2^{p_i} e^{-(\alpha_i+\Delta_{ki}+1/\lambda_i)} \quad (2)$$

where N and M are the number of nearest-neighbors (NN) and next-nearest neighbors (NNN) at distances R_1 and R_2 (in the equivalent crystal), respectively), r denotes the distance between the reference atom and its neighbors, $S(r)$ describes a screening function, and the sum runs over NN and NNN. A matrix of perturbative BFS parameters, Δ_{ji}, describes the changes in the electron density in the vicinity of atom i due to the presence of an atom j (of a different chemical species), in a neighboring site. The single element parameters describing any arbitrary reference state for a given atom are related to the equilibrium values for r_{WSE}, the cohesive energy, E_c, and the bulk modulus, B_0, (or the scaling length l, used to replace B_0 in order to allow for a closer correspondence with the universal binding energy relationship [10] (UBER)). Additional ECT parameters (p, l, α, and λ) are derived from them [9]. These equations are used for the calculation of the lattice parameter a^S or a^C of a perfect crystal where the reference atom i has the same energy as it has in the geometrical environment of the alloy under study. Once the lattice parameter of the strain or chemical equivalent crystal are determined, the BFS contribution to the strain or chemical energy are computed using the UBER, which contains all the relevant information concerning a single-component system. Finally, the BFS strain and chemical energy contributions are linked by a coupling function g_i, which describes the influence of the geometrical distribution of the surrounding atoms in relation to the chemical effects and is given by $g_i = \exp(-a_i^{S*})$.

The BFS parameters are determined from FP calculations by using the full potential linearized augmented plane wave (FLAPW) method, as implemented in the WIEN2K package [11], but their validation depends on their ability to describe basic known features of the binary combinations of these elements. Unlike other systems for which there is abundant theoretical or experimental information, the background available for U-X compounds (X = Al, Si, Mo, Ge) is very limited. The validity of the parameters are tested against basic structural information and experimental data available in the literature. For example, in the UMo system we checked the Dwight measurement [12] of the UMo solid solution lattice parameter versus Mo: $a(x)/a_U = 1 - 0.0009021x$ (x in at%Mo) content for the range 12.7 to 35.5 at.% Mo at 1173 K. The BFS prediction, is $a(x)/a_U = 1 - 0.0009044x$, in excellent agreement with the Dwight's results.

3. Role of additives in the Al/U and Al/UMo interface

The BFS-based methodology assumes no a priori information on the system at hand and none of the experimental information that could be possibly available is used in the formulation and application of the method. The only input necessary consists of the lattice structures and the parameterization of the participating elements provided by FLAPW calculations. Although in this work the calculations are restricted to a rigid bcc cell with the lattice parameter of the U portion, it is also true that for the purpose of this study, focused on determining qualitative trends and changes in behavior for different additives, the proposed framework is largely appropriate. It should also be noted that the low temperature results are a consequence of the simulation scheme used, based on a Monte Carlo - Metropolis algorithm where atoms ‘diffuse’ based only on the

energetics of the initial and final state, and not due to their ability to overcome diffusion barriers. In other words, the simulation results just say that there are lower energy accessible states to which the system can evolve, but accurate diffusion rates can only be obtained if diffusion barriers are properly taken into account. In spite of these limitations, if the parameterization and general modeling scheme is correct, it is possible to obtain information on general trends and the driving forces for the processes found experimentally.

3.1 The role of Mo in Al/U interface

The experimental results for Al/(U,Mo) show that the U-2 wt% Mo/Al dispersions increase in volume by 26% at 673 K after 2000 h. This large volume change is mainly due to the formation of voids and cracks resulting from nearly complete interdiffusion of U-Mo and Al. Fuel particles containing 4 wt% Mo reacted extensively with the matrix aluminum during fuel fabrication and irradiation but fuels with 6 wt% or more Mo content performed well during irradiation, exhibiting low to moderate fuel/matrix interaction and stable fission gas bubble growth [1-3]. Others experimental results show that the U–7 wt% Mo alloy previously homogenized retains the γ-(U,Mo) phase, and the formation of $(U,Mo)Al_3$ and $(U,Mo)Al_4$ at 853 K is observed [3].

In spite of the rigid cell limitation in the simulations, based on a bcc cell with a lattice parameter characteristic of the U-Mo portion of the cell, it is possible to gather the necessary information to understand the behavior of Al in terms of Mo concentration. Fig. 2 shows concentration profiles obtained through MC simulations using BFS method for the atomic energetics for Al/U-5 wt% Mo and Al/U-5 wt% Mo. The results indicate reduced diffusion of Al in U-Mo relative to the binary Al/U case. The effect of Mo on Al diffusion can be observed at 400 K, where substantial differences between cells with 5 and 10 wt% Mo can be seen. In the first case, Al diffuses to layers far from the interface, with barely 20% in its vicinity. For 10 wt% Mo, however, Al preferentially goes to regions near the interface with low Mo concentration. Far from the interface, Al concentration at 400 K varies from 50% for pure U, 15% for U-5 wt% Mo, to nearly zero for U-10 wt% Mo. The simulations and the concentration profiles at T = 400 K also reveal that Al and Mo show a tendency toward compound formation. However, this effect could also be understood as a result of Al diffusion to Mo-defficient regions which, statistically, populates sites in the vicinity of Mo atoms. Either way, the Al and Mo count would show peaks and valleys of the same nature in the concentration profiles. These results show that the ‘stopping power’ of Mo for Al interdiffusion is limited, resulting in the formation of interfacial ternary compounds of varying composition, depending on their location relative to the interface.

3.2 The role of Si in the Al/U interface

There is no experimental evidence for this system. It is in cases like this where it is important to fill the knowledge gaps with modeling results that assure consistency with known cases. More importantly, analyzing every possible situation with the same modeling scheme allows us to gain detailed insight on the role played by each atomic species and the interactions between them. The MC simulations show that Si additions to the Al matrix have a striking effect even in the basic case (Al/U). The results for this system, shown in Fig. 3, can be summarized with two distinct examples, namely, Al-5 wt% Si/U and Al-10 wt% Si/U, for which simulations were performed in the range $1 < T < 400$ K. In contrast with the Al/U system, Al diffusion in U is drastically affected by Si. The simulations show higher diffusion rates for Si than for Al. As shown in Fig. 3 for T = 190 K, Si inhibits Al interdiffusion at low temperature. This effect is more noticeable in

regions with higher Si concentration. As T increases, Si diffuses to deeper layers allowing for Al diffusion to the interfacial region. There is a noticeable difference between the 5 and 10 wt% Si in Al cases, as seen in Fig.3, but both show Al depletion in near-interfacial regions and the formation of ordered compounds where Si is in the majority. For 10 wt% Si in Al, there is a noticeable effect in the diffusion of Al to U mainly in the regions where Si is in the majority. The simulations show that the diffusion path of Al is through Si-poor regions (particularly for T = 400 K), or where U-Si precipitates disappear.

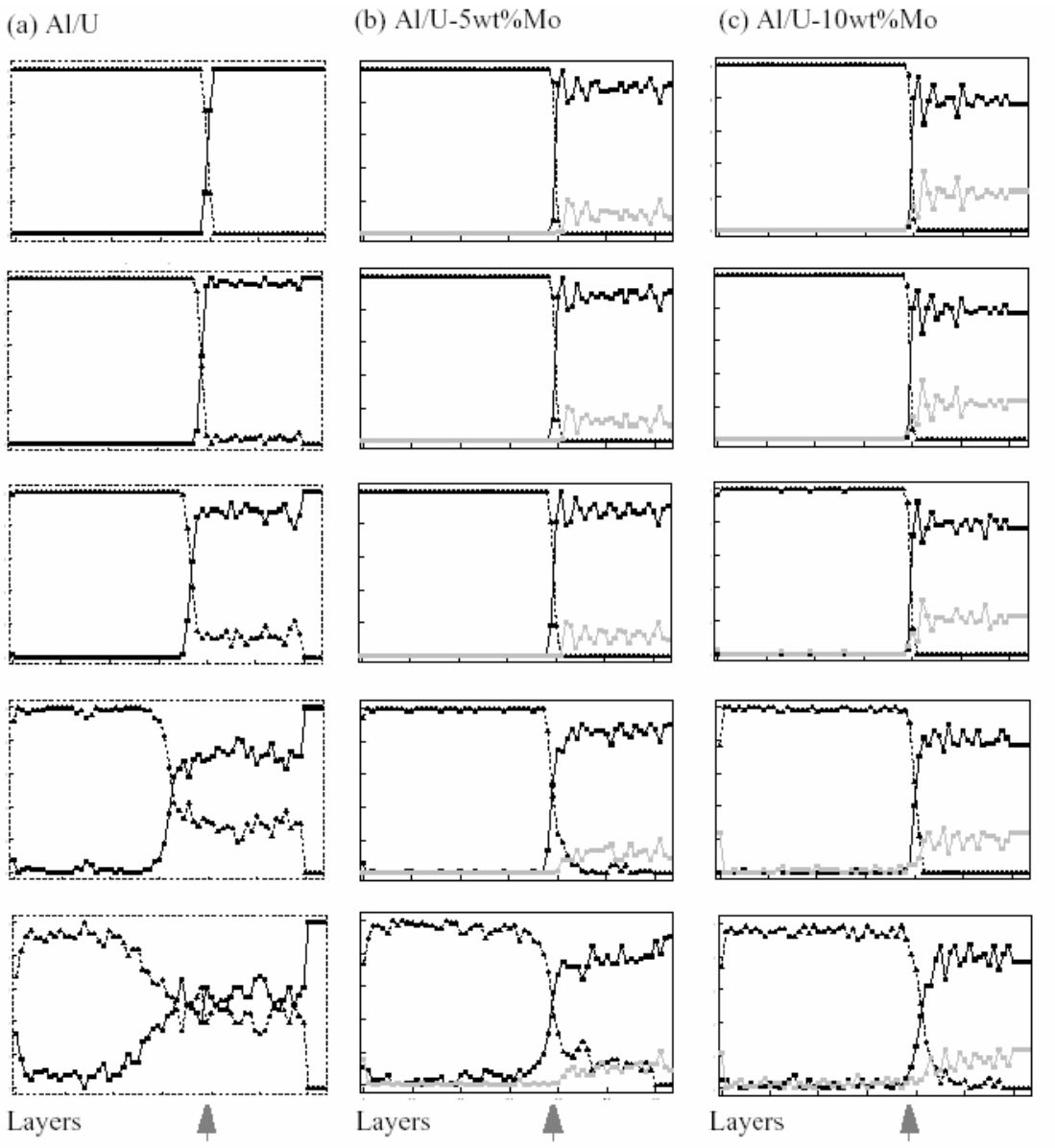

Figure 2. Composition profiles of the computational cells representing (a) the interfacial region between Al and U, (b) Al and U-5 wt% Mo, and (c) Al and U-10 wt% Mo. The composition profiles, from left to right, denote the changes of concentration (in at%) in each plane in the vicinity of the interface. The different plots, from top to bottom, indicate the stable profiles at 90, 140, 190, 300 and 400 K. U and Mo profiles are indicated with solid black and grey lines, respectively. Al is indicated with a dashed line. The arrow indicates the original interface location.

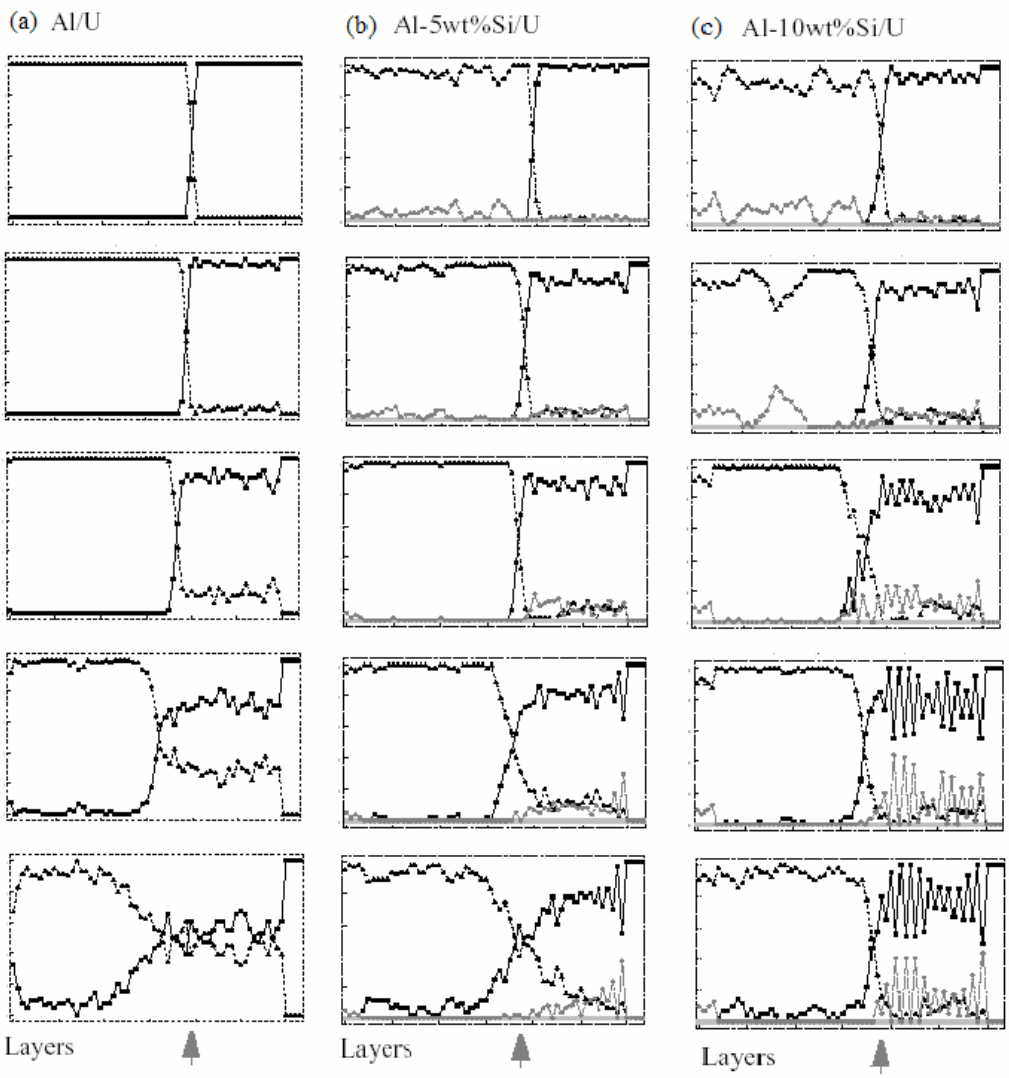

Figure 3. Composition profiles of the computational cells representing (a) the interfacial region between an Al-5wt%Si and U, and (b) Al-10wt%Si and U. The composition profiles, from left to right, denote the changes of concentration (in at%) in each plane in the vicinity of the interface. The different plots, from top to bottom, indicate the stable profiles at 90, 140, 190, 300 and 400 K. U profiles are indicated with black solid lines. Al and Si profiles are indicated with black (dashed) and grey (dot-dashed) lines. The arrows indicate the original interface location.

3.3 The role of Si in the Al/UMo interface

Experimental results suggest that Si additions to Al introduce important changes in relation with the phases found inside the interaction layer: $(U,Mo)(Al,Si)_3$ near the Al alloy, a two-phase zone consisting of $(U,Mo)(Al,Si)_3$ and, probably, $(U,Mo)(Al,Si)_{2-x}$ near U-Mo alloy. No $(U,Mo)Al_4$ was found [3]. $(U,Mo)(Al,Si)_3$, which is the main component of the interaction layer, is the phase reported as the interaction product in dispersion Si fuel elements. The simulations shown in Fig. 4 address the simultaneous effect of adding Si to Al and Mo to U, their influence in the structure of the interface, and in the interactions between the two alloying additions. The trends observed in the ternary case Al/UMo are, to a certain extent, conserved. The most striking result, due to the interaction between all four elements, is the complete depletion of Si in Al regions close to the interface, an effect that is in excellent agreement with experiment.

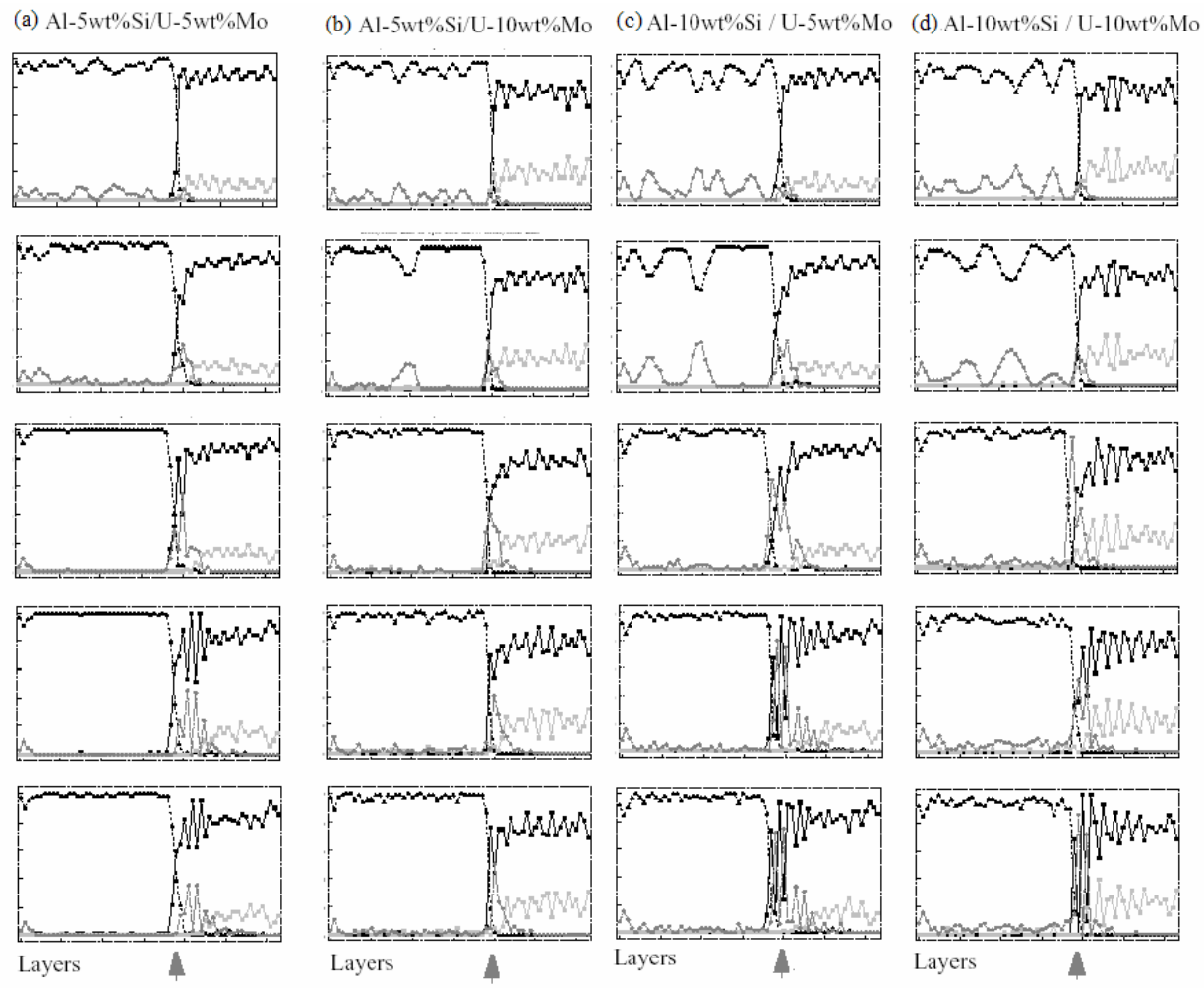

Figure 4. Composition profiles of the computational cells representing (a) the interfacial region between an Al-5wt%Si and U-5wt%Mo, (b) Al-5wt%Si and U-10wt%Mo, (c) Al-10wt%Si and U-5wt%Mo, and (d) Al-10wt%Si and U-10wt%Mo. The composition profiles, from left to right, denote the changes of concentration (in at%) in each plane in the vicinity of the interface. The different plots, from top to bottom, indicate the stable profiles at 90, 140, 190, 300 and 400 K. U and Mo profiles are indicated with black and grey solid lines, respectively. Al and Si profiles are indicated with black (dashed) and grey (dot-dashed) lines. The arrows indicate the original interface location.

Results for Al-5 wt% Si and for Al-10 wt% Si (Fig. 4), reproduce the main features of the experimental results, highlighting a strong trend towards the formation of interfacial compounds. As mentioned above, working on a rigid bcc cell prevents us from properly determining the structure and composition of these compounds, but does not hinder the fact that their formation strongly depends on the Si and Mo contents. Additional effects due to the interactions between the participating elements are also observed, mainly, the interaction between Mo and Si, resulting in a region free of Mo and Al where Si (in the majority) forms compounds. This effect, where Mo inhibits Si diffusion, is proportional to Mo concentration, allowing for Si-rich planes resulting in changes in the composition of the interfacial compounds from U_3Si to B2 USi. The combined effect of Si and their interactions is a noticeable decrease in Al difusión, more noticeable with increasing content of either element. Figure 5 compares experimental and BFS predictions showing the main features observed in the Al-Si/U-Mo interface.

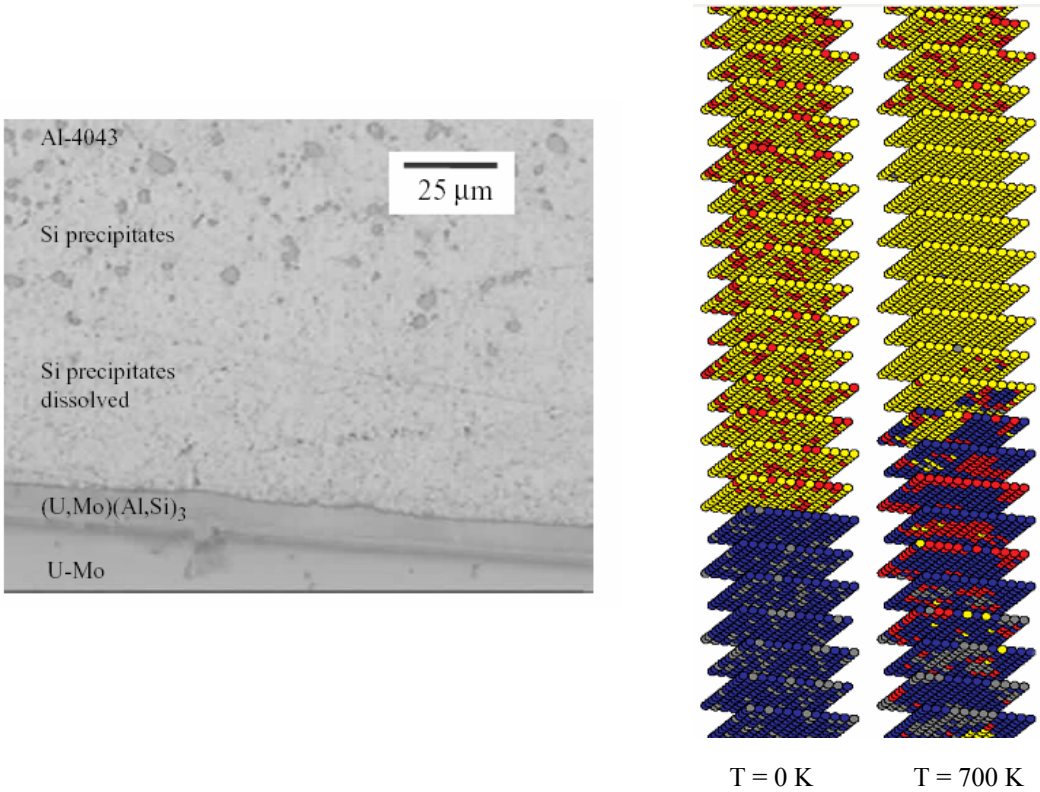

(a) (b)

Figure 5. a) Al-5.2 wt% Si/U- 7wt% Mo interdiffusion layers showing the zone of depletion of Si precipitates near the interdiffusion layer. (Reproduced with the permission of the authors). b) Simulations of 10000 atoms for Al-20wt%Si / U–10wt%Mo showing the main experimental results: Si depletion in Al side, compound formation in the zone between Al and U-Mo sides and an unexpected interaction between Mo and Si which inhibit the Si diffusion to deeper layers in the UMo solid solution thus improving the stopping power for Al diffusion.

3.4 The role of Ge in the Al/UMo interface

The observed and computed behavior of Si on Al diffusion raises questions if another element of the same group, such as Ge, present the same behavior if it is used as an additive in Al. This is yet one more case in which the lack of experimental results or any guiding evidence motivates the use of modeling in order to preview qualitative changes before proceeding to experimental verification. Therefore, we apply the same modeling tools to establish a comparison between the role of Si and Ge, with particular emphasis on the formation of metastable compounds with Al. The results of the simulations make it clear that there are noticeable differences between the behavior of Si and Ge. In contrast with the behavior of Si described above, the Ge remains mainly associated with Al, a consequence of the tendency for metastable compound formation observed experimentally in the Al-Ge system. This is rather surprising, given the many similarities between the parameterization schemes for each element. The strong tendencies for compound formation between Si and U, magnified by the interaction between Mo and Si, is not observed for Ge, which remains almost exclusively in the Al side with little Ge diffusion into U. In spite of the observed weak trends for the formation of interfacial compounds (especially at

low temperatures), no major qualitative differences are observed with respect to the pure Al case, casting doubt on the ability of Ge additions to achieve the desired effects.

4. Concluding remarks

In this work we applied the BFS method for alloys to model interfacial phenomena and show that atomistic computational modeling could become a valuable tool to aid the experimental work in the development of nuclear fuels through the understanding of basic features observed in the Al/UMo interface and the effect of additives to the Al matrix. This work provides the first attempt to tackle some issues in an oversimplified modeling framework. However, several questions remain unanswered, as are the crystallographic nature of the interfacial compounds that form or how small quantities of alloying additions both in the matrix or fuel particles can influence the formation of these compounds and their effect in the overall behavior of the system. However, in spite of the fact that all the calculations refer to a rigid environment where both the Al matrix and UMo particles are represented by a bcc lattice characteristic of the UMo fuel, the basic features characterizing the real system can still be identified: 1) the increased Al/UMo interdiffusion with temperature, 2) the Al stopping power of increasing Mo concentration, and 3) the formation of interfacial compounds. Moreover, significant results were also obtained in the case of Si additions to Al, once again reproducing the main features observed experimentally: 1) the trend indicating formation of interfacial compounds, 2) much reduced diffusion of Al into UMo due to the high Si concentration, 3) Si depletion in the Al matrix, and 4) an unexpected interaction between Mo and Si which inhibit Si diffusion to deeper layers in the UMo solid solution thus improving the stopping power for Al diffusion. Also, the role of another element, Ge, of the same group as Si, was investigated. In contrast with Si, we observed a weak tendency to compound formation and, basically, no differences were observed in Al difussion with respect to pure Al. As no experimental results or guiding evidence are available for the system Al-Ge/U-Mo, this is a good example of how modeling could help to understand the behavior of the system before proceeding to experimental verification.

5. References

[1] G. L. Hofman, M. R. Finlay and Y. S. Kim, RERTR-4 and 5, International Meeting on RERTR, November 7-12, 2004, Vienna, Austria.

[2] P. Lemoine, F. Huet, B. Guigon, C. Jarousse and S. Guillot, International Meeting on RERTR, November 7-12, 2004, Vienna, Austria.

[3] M. I. Mirandou, S. N. Balart, M. Ortiz and M. S. Granovsky, J. Nucl. Mater. 323, 29 (2003).

[4] G. Bozzolo and J. E. Garcés, in Atomistic modeling of surface alloys, Surface alloys and alloy surfaces, The Chemical Physics of Solid Surfaces, Vol. 10, Elsevier (2002).

[5] G. Bozzolo, J. Khalil, M. Bartow and R. D. Noebe, Mat. Res. Soc. Symp. Proc. 646, N6.2 (2001).

[6] A.Wilson, G. Bozzolo, R. D. Noebe and J. Jowe, Acta Mater. 50, 2787 (2002).

[7] G. Bozzolo, R. D. Noebe and H. Mosca, J. Alloys Compd. 386, 125 (2005).

[8] J. E. Garcés and G. Bozzolo, Phys. Rev. B 71, 134201 (2005).

[9] J. Smith, T. Perry, A. Banerjea, J. Ferrante, and G. Bozzolo, Phys. Rev. B 44, 6444 (1991).

[10] J. H. Rose, J. R. Smith, and J. Ferrante, Phys. Rev. B 28, 1835 (1983).

[11] P. Blaha, K. Schwartz, and J. Luitz, WIEN97, T.U. Wien, Improved and updated Unix version of the copyrighted WIEN code; P. Blaha, P. Schwartz, P. Sorantin, and S. B.Trickey, Comput. Phys. Commun. 59, (1990) 399.

[12] A. E. Dwight, J. Nucl. Mater. 2, 81 (1960).